RSC Advances

Synthesis of diallyl disulfide (DADS) induced gold nanoparticles: characterization and study of its biological activity in human leukemic cell-lines

Journal:	*RSC Advances*
Manuscript ID:	RA-ART-11-2014-015388.R1
Article Type:	Paper
Date Submitted by the Author:	15-Jan-2015
Complete List of Authors:	Dasgupta, Pritha; University of Calcutta, Biophysics, Molecular Biology and Bioinformatics Bhattacharya, Abhishek; University of Calcutta, Biochemistry Pal, Rajat; University of Calcutta, Biophysics, Molecular Biology and Bioinformatics Dasgupta, Anjan; University of Calcutta, Biochemistry Sengupta (Bandyopadhyay), Sumita; University of Calcutta, Biophysics, Molecular Biology and Bioinformatics

SCHOLARONE™
Manuscripts

Synthesis of diallyl disulfide (DADS) induced gold nanoparticles: characterization and study of its biological activity in human leukemic cell-lines

Pritha Dasgupta[1], Abhishek Bhattacharya[2], Rajat Pal[1], Anjan Kumar Dasgupta[2] and Sumita Sengupta (Bandyopadhayay)[1]

[1]*Department of Biophysics, Molecular Biology and Bioinformatics, University of Calcutta,* 92 A.P.C. Road, Kolkata 700009, India
[2]*Department of Biochemistry, University of Calcutta,* 35 Ballygunge Circular Road, Kolkata-700 019, India

Correspondence: Sumita Sengupta (Bandyopadhyay)
Department of Biophysics, Molecular Biology and Bioinformatics,
University of Calcutta,
Email: ssbmbg@caluniv.ac.in

Abstract

Novel approaches of nanoparticle synthesis using herbal products and its potential application in treatments are now in the limelight of recent cancer research. Diallyl disulfide (DADS), a bioactive component of garlic has been used for centuries as an effective remedy for different ailments including cancer. In the present study, DADS is used to synthesize less toxic, eco-friendly gold nanoparticles having anti-proliferative effects against cancer cells. DADS induced gold nanoparticles (D-GNPs) display characteristic surface plasmon band near 551 nm which is 22 nm red shifted compared to conventionally prepared gold nanoparticles (GNPs) using tri-sodium citrate. Moreover, hydrodynamic diameter of D-GNP ranges from 70 to 77 nm and zeta potential of -24.6 mV. A nearly spherical ultra-structure of D-GNPs was visualized under Atomic Force Microscope and Transmission Electron Microscope. FT-IR analysis confirms the association of sulfur group of DADS with these nanoparticles. D-GNPs show dose dependent cytotoxicity in human leukemic cell-lines U937 and K562. Cellular uptake of D-GNPs in U937 leading to nuclear fragmentation and DNA ladder formation are other insightful findings. This report therefore details the synthesis of stable gold nanoparticles using DADS and reveals D-GNPs to be highly effective anti-proliferative agent showing apoptosis in human leukemia cell-lines.

Keywords: Cytotoxicity, apoptosis, DADS induced gold nanoparticle (D-GNP), Surface plasmon resonance

1. Introduction

For the last two decades nanoscience and nanotechnology has advanced the field of research by focusing on new nanomaterials discovery and exploring their new applications, especially in electronics, information technology, sensor development, catalysis, and biomedical sciences[1–5]. Lately, nanotechnology has piqued the interest of medical community for use in biomedicines. Nanoparticles are engineered as nano-platforms for effective and targeted drug delivery with interest in *in-vitro* diagnostics, novel biomaterial designing, bio-imaging, therapies and active implants[6–10]. The important step in the field of nanotechnology is to develop eco-friendly nanoparticles for safer use in modern treatments.

Cancer is a public health problem worldwide with a hazardous death rate. Treatment of cancer is thus in a demand for new drugs, new therapies and techniques which would surely improve sufferings of cancer patients. Intelligent design of engineered nanoparticles made it exceptionally promising agent in cancer therapeutics. Interestingly, gold nanoparticles (GNPs) grab our attention in this regard for several reasons. First, they are easily prepared. Additionally, GNPs have strong binding affinity towards thiols, disulfides and amines which facilitates its conjugation with biomolecules like DNA, proteins, receptors *etc*[11–15], and thereby made GNP a potential tool for cancer treatment and site specific drug delivery[16–19]. Gold nanoparticles also exhibit unique physiochemical properties which include surface plasmon enhanced absorption and scattering [20,21] that make GNPs important for bio-imaging [22]. GNPs are not susceptible to photo-bleaching and are very much biocompatible in human cells. Bio-conjugation and bio-modification of GNPs is the subject of intense research in the recent years which make it potent for cancer diagnosis and therapeutics[23].

Biosynthesis of metal nanoparticles using plant extract has achieved exceptional attention as a simple alternative to chemical procedures in recent years. Unlike chemical techniques, biosynthetic method is more facile, eco-friendly resulting in less toxic, bio-compatible nanoparticles. Gardea-Torresdey *et al* (2002) first reported the biosynthesis of metal nanoparticles by plant products[24]. Several reports described biosynthesis of metal nanoparticles by plant leaf extract and their potential application in several studies[25–34]. They specially emphasized the bio-reduction of chloroaurate ions and silver ions by geranium leaf extract[26,27] and neem leaf extract [28]. Synthesis of gold nanotriangles is also reported by the same group of researchers using lemon grass extract [29] and tamarind extract[31]. There are handful of other reports elucidating synthesis of gold and silver nanoparticles using plant extract like aloe-vera, cinnamon, garlic *etc*[30,34–37]. Most of the aforementioned research on the synthesis of gold and silver nanoparticles utilized plant extracts *i.e.*, broths resulting from boiling fresh plant leaves as the reducing agent. In the present study, a unique challenge of using an active component of herbal products, previously unexploited for bio-reduction, has been used to synthesize stable gold nanoparticles. Diallyl disulfide (DADS), the active component of garlic, has been found to inhibit proliferation of different cancer cells including leukemia in a multi-targeted way[38–42]. In our previous study[42], we have explicitly illustrated the anti-proliferative mechanism of DADS in leukemic cell-lines with special emphasis on p21 and NFκB. DADS was found to induce intrinsic apoptosis where NF-κB dependent $p21^{waf1/cip1}$ induction played significant role in transient G2-M arrest. Increasing the efficacy of cytotoxic activity of DADS was therefore of great concern and the challenge was taken to use only DADS for the purpose of synthesis of stable gold nanoparticles without involving any other stabilizing agents with the aim of preparing more efficient anti-proliferative agent.

In this study we have utilized a single-step approach for the synthesis of gold nanoparticles in aqueous solution using a medicinally important organosulfur component of garlic. Although garlic extract has been used to prepare size controlled synthesis of gold nanoparticles[36] but to the best of our knowledge this is the first report involving use of active garlic components, like diallyl disulfide in an environmental-friendly method for the aqueous synthesis of stable gold nanoparticles. DADS induced gold nanoparticles (D-GNPs) have been physically characterized and the biological activities of these D-GNPs in leukemic cell-lines are also elucidated.

2. Results and discussion

2.1. Preparation of D-GNPs and its analysis by UV-visible absorption spectroscopy

Preparation of gold nanoparticles has been carried out by boiling 10 ml of 0.01 % $HAuCl_4$ in presence of different volumes of 50 mM DADS (diluted in DMSO). Here, DADS is acting as both reducing agent and stabilizer of gold nanoparticles produced by this bio-synthetic method. Change in color from colorless to violet color of different intensities depending upon the amount of DADS used is observed when the solution was heated for 5 min. The change in color suggests formation of gold nanoparticles as seen in Figure 1a where, gold nanoparticles prepared by addition of 2.5 µl, 5 µl, 10 µl and 15 µl of 50 mM DADS are designated as D-GNP-I, D-GNP-II, D-GNP-III, D-GNP-IV respectively. On the other hand, gold nanoparticles (GNP) prepared by conventional method of reduction of chloroauric acid by trisodium citrate produced wine red colored particles.

The reduction of $HAuCl_4$ and the formation of gold nanoparticles (D-GNP) are monitored by observing the changes in absorption spectra originating from the surface plasmon resonance of the D-GNPs using UV–visible spectrometer as shown in Figure1b. None of the ingredients *i.e.,* DADS or chloroauric acid have any absorbance, whereas, when these two ingredients are boiled

together for only 5 mins, a characteristic pattern of surface plasmon absorption peak at 551 nm is seen indicating formation of nanoparticles. On the other hand, gold nanoparticles (GNP) formed by conventional method by reducing chloroauric acid with trisodium citrate shows surface plasmon absorption maxima at 529 nm. A spectral shift of 22 nm is observed for D-GNP as compared to GNP indicating the gold nanoparticles that are formed using DADS are larger and less spherical than those formed by using citrate (GNP). Interestingly, a characteristic new absorption peak is observed in the UV region (at around 295-300 nm) in case of D-GNPs which is not present in case of GNP (shown in the inset).

2.2. Physical characterization of DADS induced gold nanoparticles (D-GNPs):

2.2.1. Determination of particle size and surface charge of D-GNPs

For physical characterization of newly formed nanoparticles synthesized by DADS, hydrodynamic volume and surface charge are measured. Dynamic light scattering (DLS) sizing detects the hydrodynamic diameter of the particles and particle agglomerates. In our experimental condition, the average hydrodynamic diameter of the gold nanoparticle (D-GNP-III) is found to be 76.42 nm when measured by DLS method. Size distribution curves show larger size of the gold nanoparticles formed by DADS (Figure 2a) as compared to the gold nanoparticles prepared by conventional method using citrate, which is found to be 31.78 nm (data not shown). Poly-dispersity index (PDI) represents the heterogeneity in size of the particles. It is evident that D-GNP-III has lower PDI values of 0.429 as compared to the gold nanoparticles prepared by conventional method using citrate (0.509), therefore has smaller variability in particle size.

The surface charge of the DADS induced gold nanoparticles are found to be -22.6 mV for D-GNP-III (Figure 2b) whereas, citrate coated GNP shows zeta potential around -20.8 mV (data not

shown). Measurement of zeta potential indicates that the surface charge of gold nanoparticles prepared by DADS is comparable to that of the gold nanoparticles prepared by conventional method.

2.2.2. External Morphological Study of gold nanoparticles

Morphology of D-GNPs has been studied by Atomic Force microscopy (AFM) and Electron microscopy (TEM). Figure 2c shows AFM images of the gold nanoparticles synthesized by 10 µl of 50 mM of DADS (D-GNP-III). 15 particles are randomly chosen from the microscopic field for diameter measurement and the diameter is found to be 62.93 ± 3.48 nm. Figure 2d represents transmission electron microscopic images of gold nanoparticles. The particle size of D-GNP-III as measured from the TEM images is found to be 62.76 ± 3.034 nm. 20 particles are randomly chosen from the microscopic field for diameter measurement. There lies a difference in the particle size as measured by AFM, TEM from that of DLS. This is because of the fact that, DLS method shows the hydrodynamic diameter of the nanoparticles whereas AFM and TEM measure the exact diameter of the nanoparticles. Apart from the particle size, an idea of the particle shape is also obtained from the AFM and TEM images of D-GNPs and it is assumed to be slightly non spherical.

2.2.3. FT-IR analysis of DADS and D-GNPs

Atoms are always in a complex interaction within a molecule. IR spectroscopy is associated with vibrational energy of atoms or group of atoms in a molecule and so IR absorption of different functional groups vary showing characteristic band pattern in IR spectrum. The FT-IR spectra of DADS and D-GNP are shown in Figure 3 and all the bands are listed in Table1. In the IR spectrum of DADS, the band present at 2929 cm^{-1} indicates C-H stretching and that at 1635 cm^{-1}signifies alkenyl C=C stretch. Similar bands are found in the IR spectrum of D-GNP indicating

the presence of same C-H stretching at 2926 cm^{-1} and alkenyl C=C stretch at 1632 cm^{-1}. C-S stretch as indicated by band position 719cm^{-1} in IR spectrum of DADS is also seen in the D-GNP IR spectrum at 714 cm^{-1} [43,44]. Moreover, bands at 1427 cm^{-1} and 1424 cm^{-1} are identified in the IR spectrum of D-GNP and DADS respectively indicating C-H symmetrical or asymmetrical bend. Interestingly, a band at 579 cm^{-1} which is found in DADS IR spectrum signifying C-S-S-C bend is totally absent in the IR spectrum of D-GNP whereas a completely new band appears at a position 1160 cm^{-1} indicating S=O symmetrical stretch. Apart from these, there is one more characteristic band at 986 cm^{-1} in the IR spectrum of DADS signifying C-H out of plane bend. This means some common characteristic bands are found to be present in both the spectra where as some characteristic bands are also there in IR spectrum of DADS which are absent in the IR spectrum of D-GNP and *vice versa*. From these results, it can be inferred that DADS is no more in its original form in D-GNP. Most probably, disulfide linkage of DADS has been oxidized for reducing $HAuCl_4$ to synthesize gold nanoparticles. The oxidation of disulfide bond is confirmed by the band at 1160 cm^{-1} indicating the presence of S=O on the surface of the nanoparticle. Uptake of oxygen by the sulfur molecule may be from the water molecules present in the reaction medium. From these it can be assumed that DADS reduces $HAuCl_4$ to form nanoparticle and oxidizes itself to produce mono allyl sulfide group which is presumably tagged on the D-GNP surface in the oxidized form.

Table 1: FT-IR bands and responsible chemical group of DADS and D-GNP

Bands (cm^{-1})	**DADS**	**D-GNP**	**Responsible chemical group**
2929 2926	Present -	- Present	C-H Stretching
2852	Absent	present	$-CH_3$ stretching
1635 1632	Present -	- Present	Alkenyl C=C stretch

1427 1424	- Present	Present -	C-H symmetrical/ asymmetrical bend of CH_3 group or H-C-H stretch
1160	Absent	Present	S=O symmetrical stretch
986	Present	Absent	C-H out of plane bend
719 714	Present -	- Present	C-S stretch
579	Present	Absent	C-S-S-C bend

2.2.4. Stability of DADS induced gold nanoparticles (D-GNPs)

DADS induced gold nanoparticles are synthesized to study its anti-proliferative potential in cancer cells. Its stability in aqueous solution or cell culture media for the entire time period of treatment is of great concern. To check the stability of DADS induced gold nanoparticles, UV-VIS spectroscopic and DLS studies has been carried out after incubating the gold nanoparticles in aqueous medium for 24 hours. Size distribution of the D-GNPs as revealed by DLS study shows that the size of the nanoparticles became 90.56 nm and 100.8 nm for D-GNP-II and D-GNP-III respectively after 24 hours in RPMI media (Figure 4a & b), whereas, the size of the particles are 70.35 nm and 76.42 nm for D-GNP-II and D-GNP-III respectively when measured immediately after synthesis. This increase in size could be due to agglomeration of the particles in cell culture medium. Moreover, UV-Vis spectra of GNP taken after 24 hours of preparation shows surface plasmon absorption peak at 532 nm whereas the same for D-GNP-II and D-GNP-III were 556 nm and 558 nm respectively (when measured after 24 hours) as seen in Figure 4c. Comparative study of surface plasmon absorption peak of freshly prepared particles to that of particles after 24 hours of preparation shows a little shift (red shift of 5 to 7 nm) in the peak values indicating slight tendency of agglomeration.

2.3. Biological activities of D-GNPs in human leukemic cell lines

2.3.1. Effects of D-GNP in human leukemic cell lines

The cytotoxic effects of the DADS induced gold nanoparticles, D-GNP-III on U937 and K562 cells is determined by trypan blue dye exclusion test. It is found that the number of viable cells decreases with increasing concentrations of D-GNP-III at 24 hours compared to the untreated cells and maximum equivalent volume of conventionally prepared gold nanoparticles *i.e.,* GNP (Figure 5a). Effects of 50μM and 100μM DADS has also been shown to compare the anti-proliferative efficacy of DADS and D-GNP-III. After 24 hours, IC_{50} values for D-GNP-III on U937 and K562 cells are found to be 14.164 ± 0.62 μM and 15.82 ± 0.798 μM respectively whereas, IC_{50} values of DADS were 58.34 ± 3.04μM, 74.02 ± 2.75μM in U937 and K562 cells respectively (almost similar to our previous report[42]). This result signifies D-GNP-III as more efficient anti-proliferative agent than DADS and the efficacy has been found to increase by 4 fold and 4.5 fold in U937 and K562 cells respectively.

2.3.2. Studies of the mode of cell death in U937 cells by D-GNP treatment

It is found that gold nanoparticles prepared by DADS (D-GNP) are efficient as an anti-proliferative agent in human leukemic cell-lines U937 and K562. Thus to elucidate the mode of cell death by D-GNP treatment, morphological changes are monitored under microscope. U937 cell-line has been chosen as a model cell-line for this purpose. U937 cells exhibits slight morphological changes when exposed to D-GNPs for 24 hours. The phase contrast microscopic pictures of U937 cells treated with 8.84 μM of D-GNP-II and 16.6 μM of D-GNP-III reveal some altered morphology as compared to control cells *i.e.,* formation of some ultra-structures and biochemical features as indicated by arrow in Figure 5 g, h, i. Moreover, D-GNP treated U937 cells when stained with DAPI shows multi-nucleation as compared to control cells (Figure 5 d, e, f). These phenomena are characteristics of apoptosis which is further supported by the

formation of inter-nucleosomal DNA fragmentation in D-GNP treated U937 cells (Figure 5 j). Thus, these results clearly indicate that D-GNP induces apoptosis in leukemic cells.

2.3.3. Cellular uptake of D-GNP in U937 cells.

Since D-GNP is found to be a potent inducer of apoptosis in U937 cells, so, it is an obvious curiosity to check whether these D-GNPs are getting inside the treated cells or not. D-GNP treated U937 cells are visualized under confocal microscope and were scanned tomographically by Z-scanning method (optical slicing along Z-axis) in order to get images of different layers of the treated cells as seen in Jose *et al*[45]. The images obtained by Z-scanning showed some black dots (as indicated by arrow) inside the cells treated with D-GNPs for 24 hours (Figure 5c), whereas, no such dark spot are visible in case of the untreated U937 cells (Figure 5b). Moreover, uptake of D-GNP-III within the cells increased both in time and dose dependent manner. Confocal images showed more incorporation of D-GNP-III aggregates in 24 hour as compared to 5 hour of D-GNP-III treated cells (figure S1e, S1f). Results shown in supplementary figure (figure S1a/b/c/d) indicated presence of increasing amount of particulate matters in U937 cells when treated with increasing concentrations of D-GNP-III as measured by the amount of side scattering (SSC-A, y-axis) by FACS[46]. Therefore, all these results confirmed the presence of D-GNPs inside the cells.

Comparing the confocal images of GNP and D-GNP-III treated U937 cells, several dark spots (nanomaterials in aggregates) were noticed for D-GNP-III (figure S1g) and GNP treated cells (figure S1h). Although presence of conventionally prepared gold nanoparticles (GNP) were seen within the cells, but GNPs could not cause noticeable decrease in cell viability even after 24 hours of treatment (as shown in figure 5a).

2.3.4. Study of intrinsic fluorescence of D-GNP treated cells

Interestingly, when D-GNP-III treated U937 cells were visualized under confocal microscope intense green punctuated fluorescence was observed as shown in Figure 6d, which were found to be absent in untreated control cells (Figure 6b) and DADS treated U937 cells (data not shown). Figure 6a and 6c represent corresponding phase contrast images of untreated and D-GNP-III treated U937 cells respectively. This intrinsic fluorescence of the D-GNP-III treated cells are also seen in the confocal images of different layers (done by Z-scanning) of D-GNP treated cells (Figure 6e, 6f, 6g, 6h).

3. Experimental Section

3.1. Materials

DADS was purchased from Fluka Chemika Co. (Bucha, Switzerland), Triton-X from Hi-Media (Mumbai, India), RPMI-1640, Fetal Bovine Serum, penicillin-streptomycin and amphotericin-B were purchased from Pan Biotech (Germany). Gold chloride and trisodium citrate were purchased from SRL (Mumbai, India). DAPI was obtained from Sigma-Aldrich (St. Louis, MO, USA). All other chemicals and reagents were of analytical grade and purchased locally.

3.2. Preparation and concentration calculation of DADS induced gold nanoparticles

DADS induced gold nanoparticles (D-GNP) were prepared by the addition of different volumes (2.5-15 µl) of 50 mM of DADS in DMSO to 10 ml of 0.01 % chloroauric acid under boiling condition (for 3-5 min). Gold nanoparticles (GNP) were formed by reducing 10 ml of 0.01 % chloroauric acid by 100µl of trisodium citrate (1%) under boiling condition[47,48]. D-GNPs (immediately after preparation) were centrifuged at 21,000 r.c.f. for 20 mins at room temperature. The precipitate was then washed twice with double distilled autoclaved water by

centrifugation as mentioned above, and then dissolved in same volume of double distilled autoclaved water before doing all experiments.

Concentration of D-GNPs were calculated using an established method[49,50] considering a part of gold from HAuCl4 was reduced by DADS during the method of preparation. Concentration of D-GNP-II and D-GNP-III were found to be 53.05μM and 100μM respectively.

3.3. UV-Visible spectral analysis

Absorption spectra of GNP and D-GNPs were recorded in the wavelength region ranging from 250 nm to 700 nm using a double beam spectrophotometer (Evolution 300, UV-Vis, Thermo Scientific).

3.4. Measurement of particle size and surface charge

The hydrodynamic diameters of gold nanoparticles were measured by Dynamic Light Scattering (DLS) using Zeta SizerNano Series-Nano ZS (Malvern Instruments). Poly Dispersity Index (PDI) gives the indication of particle size distribution which was calculated as the weight average molecular weight divided by the number average molecular weight.

Surface charges of the gold nanoparticles were determined by the measurement of zeta potential using Zeta SizerNano Series-Nano ZS (Malvern Instruments). Each data point for zeta potential is an average of at least 10 measurements. Each analysis time was for 60 sec.

3.5. Morphological study of gold nanoparticle

The morphology of the gold nanoparticles was characterized by Atomic Force Microscope (Bruker AXS, Inova). GNPs prepared by different concentration of DADS (D-GNPs) were spread on glass slides pre-washed with acetone. Samples were dried under vacuum and were

measured by atomic force microscopic method. Sizes of the particles were calculated using Nanoscope Analysis software.

Morphology of gold nanoparticles induced by DADS (D-GNPs) were also visualized under Transmission Electron Microscope using FEI Model Tecnai S-twin instrument operated at an accelerating voltage of 200 KV. For TEM analysis, samples were prepared by spreading drops of the gold nanoparticle dispersions on carbon-coated copper grids. The mixtures were allowed to dry for 1 min followed by removal of the extra solution using a blotting paper.

3.6. FT-IR analysis of DADS induced gold nanoparticles

For FT-IR analysis, gold nanoparticles (immediately after preparation) were centrifuged at 21,000 *r.c.f.* for 20 mins at room temperature followed by lyophilization. The lyophilized products were taken for FT-IR studies on KBr disc using FT-IR spectrophotometer (Perkin Elmer, Spectrum-2). The scanning resolution was 4 cm^{-1} and covered a range of 450 cm^{-1} to 4000 cm^{-1}.

3.7. Cell culture

Human leukemia cell-lines U937, K562 were purchased from National Centre for Cell Science (Pune, India) and maintained in RPMI-1640 media supplemented with 10% fetal bovine serum, 100 IU/mL penicillin, 100 µg/mL streptomycin and 2.5 µg/mL amphotericin-B (Pan Biotech (Germany). The cells were cultured at 37^0C in a humidified atmosphere having 5% CO_2. For experimental purpose, cells were seeded at a density of 0.3 x 10^6/ml, incubated for 3 hours prior to D-GNP treatment.

3.8. Cell viability assay

U937 and K562 cells ($2x10^4$/ 200 µl of media) were seeded in 96 well plates, allowed for 3 hours incubation prior to treatment with DMSO (control), different concentrations DADS induced gold nanoparticles (D-GNP) for 24 hours. Cell viability was measured by counting viable cells (bright cells) under microscope after staining the treated cells with trypan blue dye. All the experiments were done in triplicate and the results were presented as means ± S.E.M.

3.9. Detection of DNA Fragmentation

U937 cells (5×10^6) were seeded, allowed for 3 hours incubation prior to treatment with different concentration of DADS induced gold nanoparticles (D-GNPs) for 24 hour. Equal numbers of cells were taken, washed with PBS, resuspended in lysis buffer (20mM Tris-HCl pH-7.4, 0.4mM EDTA pH- 8.0, 0.25% TritonX-100), incubated at room temperature for 15 min and were then centrifuged at 25,000 r.c.f at 4^0C for 10 min. DNA was precipitated with chilled isopropanol in presence of 550mM NaCl, followed by centrifugation at 25,000 r.c.f for 5 min. The precipitate was washed with 70% ethanol, dried and resuspended in TE buffer (10mM Tris-HCl, pH-8.0, 1mM EDTA), followed by RNase-A (100µg/mL) treatment, phenol:chloroform extraction and then precipitation. The DNA was again resuspended in TE buffer and was separated on 1.6% agarose-TBE gel and visualized by gel documentation system (BioRad) after staining with EtBr.

3.10. Detection of multi-nucleation by staining cellular nucleus with DAPI

U937cells (4×10^6) were treated with or without DADS induced gold nanoparticles (D-GNPs) for 24 hours, washed with PBS and fixed with 4% paraformaldehyde at room temperature for 20 mins. Cells were then permeabilized with 0.1 % TritonX-100 and stained with DAPI (2µg/mL) in dark for 5 mins at room temperature and visualized under Zeiss LSM 510 Meta confocal microscope.

3.11. Cellular uptake of gold nanoparticles

Internalization of DADS induced gold nanoparticles (D-GNPs) in U937 cells was studied by confocal microscopy. 2×10^6 cells were seeded, allowed for 3 hours incubation and then exposed to different concentration of D-GNPs for 24 hours. Cells were then collected by centrifugation, washed twice with PBS, spread over thin clear glass slides and photographed by Olympus Confocal Laser Scanning Microscope (model IX-81). To find the cellular uptake of D-GNPs, confocal microscopic study were also done by optical slicing using Z-scanning (scanning along Z-axis) in different layers of D-GNPs treated cells.

Conclusion

It has already been discussed in our previous study that diallyl-disulfide is an efficient and a potent anti-proliferative agent for human leukemic cell-lines lacking wild type p53[42]. The mechanism of action of DADS is however established in leukemic cell-lines as it is seen to mediate transient G2/M arrest through p21 induction followed by apoptosis in mitochondria mediated pathway. Thus, it has been of great interest to exploit DADS as a bio-reducing agent in the synthesis of gold nanoparticles.

Nanoscience and nanotechnology has become a new platform of cancer research where gold nanoparticle has already earned fame as popular tool for cancer treatment and therapeutics. Interestingly, we have noticed that diallyl-disulfide, a garlic component, is capable of reducing chloroauric acid to synthesize gold nanoparticles. Possibly the sulfhydryl group of DADS is responsible for the reduction of chloroauric acid into gold nanoparticles. DADS associated gold nanoparticles (D-GNPs) shows surface plasmon response peak at 551 nm. The average hydrodynamic diameter has been found to be below 100 nm and surface charge distribution is comparable to the gold nanoparticles formed by conventional method using tri-sodium citrate.

These results are in support of notion that these newly synthesized D-GNPs are indeed nanoparticles. AFM and TEM study vividly describes that, DADS induced gold nanoparticles are almost spherical in shape with diameter in the range of 62.93 ± 3.48 nm. To identify the biological activity of these D-GNPs, human leukemic cell-lines like U937 and K562 were challenged with D-GNPs. Most interestingly, the IC_{50} values of D-GNPs were found to be almost about five fold lower than that of only DADS as we have reported in our previous study[42]. Moreover, D-GNPs similar to DADS cause cellular death in human leukemic cell-lines through apoptosis. It is also noteworthy that, D-GNP treated U937 cells emit green fluorescence which could be used for imaging and targeting purposes. Thus, DADS induced gold nanoparticle formation is entirely a new approach of GNP synthesis where the gold nanoparticles thus formed are found to work more efficiently than DADS in treating leukemic cell-lines. This study also opened up scopes for future studies in revealing its anti-proliferative mechanism in different cancer cell-lines. Along with that, the most promising output of this study could be to open a new field of studies for imaging and targeting applications of D-GNPs, by using the D-GNP induced intrinsic fluorescence. Finally, D-GNP induced intrinsic fluorescence as seen from the treated cells under confocal microscope has been one of the most promising outcomes of this study which could open a new field of studies for imaging applications in future.

Acknowledgement

We are grateful to Dr. Tapas K. Sengupta for his helpful suggestions. We thank Alina Chakraborty for repeating confocal microscopic experiments, and Samares Maiti for his help in determining D-GNP concentrations. We acknowledge DST and UGC for funding and UGC (RFSMS) for providing fellowship to PD. This work was supported by grant from Center for Research in Nanoscience & Nanotechnology, University of Calcutta to SS(B).

References

1. H. Park, J. Park, A. K. L. Lim, E. H. Anderson, A. P. Alivisatos and P. L. McEuen, *Nature*, 2000, **407**, 57–60.
2. S. De Franceschi and L. Kouwenhoven, *Nature*, 2002, **417**, 701–2.
3. N. Toshima, *Macromol. Symp.*, 2008, **270**, 27–39.
4. M. C. Daniel and D. Astruc, *Chem. Rev.*, 2004, 104, 293–346.
5. J. Gao, H. Gu and B. Xu, *Acc. Chem. Res.*, 2009, **42**, 1097–107.
6. S. Eustis and M. A. el-Sayed, *Chem. Soc. Rev.*, 2006, **35**, 209–17.
7. R. Sardar, A. M. Funston, P. Mulvaney and R. W. Murray, *Langmuir*, 2009, **25**, 13840–51.
8. J. Zhou, J. Ralston, R. Sedev and D. A. Beattie, *J. Colloid Interface Sci.*, 2009, **331**, 251–62.
9. N. L. Rosi and C. A. Mirkin, *Chem. Rev.*, 2005, **105**, 1547–62.
10. D. A. Giljohann, D. S. Seferos, W. L. Daniel, M. D. Massich, P. C. Patel and C. A. Mirkin, *Angew. Chem. Int. Ed. Engl.*, 2010, **49**, 3280–94.
11. Y. Ding, J. Liu, H. Wang, G. Shen and R. Yu, *Biomaterials*, 2007, **28**, 2147–54.
12. S.-H. Huang, *Clin. Chim. Acta.*, 2006, **373**, 139–43.
13. P. Mukherjee, R. Bhattacharya, N. Bone, Y. K. Lee, C. R. Patra, S. Wang, L. Lu, C. Secreto, P. C. Banerjee, M. J. Yaszemski, N. E. Kay and D. Mukhopadhyay, *J. Nanobiotechnology*, 2007, **5**, 4.
14. T. Niidome, M. Yamagata, Y. Okamoto, Y. Akiyama, H. Takahashi, T. Kawano, Y. Katayama and Y. Niidome, *J. Control. Release*, 2006, **114**, 343–7.
15. L. R. Hirsch, N. J. Halas and J. L. West, *Methods Mol. Biol.*, 2005, **303**, 101–11.
16. P. Horcajada, T. Chalati, C. Serre, B. Gillet, C. Sebrie, T. Baati, J. F. Eubank, D. Heurtaux, P. Clayette, C. Kreuz, J.-S. Chang, Y. K. Hwang, V. Marsaud, P.-N. Bories, L. Cynober, S. Gil, G. Férey, P. Couvreur and R. Gref, *Nat. Mater.*, 2010, **9**, 172–8.
17. H. K. Sajja, M. P. East, H. Mao, Y. A. Wang, S. Nie and L. Yang, *Curr. Drug Discov. Technol.*, 2009, **6**, 43–51.
18. J.-M. Nam, C. S. Thaxton and C. A. Mirkin, *Science*, 2003, **301**, 1884–6.
19. S. I. C. , and H. T. Hyon Bin Na, *Adv. Mater.*, 2009, **21**, 2133–2148.
20. P. K. Jain, X. Huang, I. H. El-Sayed and M. A. El-Sayed, *Plasmonics*, 2007, **2**, 107–118.
21. R. A. Sperling, P. Rivera Gil, F. Zhang, M. Zanella and W. J. Parak, *Chem. Soc. Rev.*, 2008, **37**, 1896–908.
22. V. J. Mohanraj and Y. Chen, *Trop. J. Pharm. Res.*, 2007, 5.
23. A. Nel, T. Xia, L. Mädler and N. Li, *Science*, 2006, **311**, 622–7.

24. J. L. Gardea-Torresdey, J. G. Parsons, E. Gomez, J. Peralta-Videa, H. E. Troiani, P. Santiago and M. J. Yacaman, *Nano Lett.*, 2002, **2**, 397–401.
25. J. L. Gardea-Torresdey, E. Gomez, J. R. Peralta-Videa, J. G. Parsons, H. Troiani and M. Jose-Yacaman, *Langmuir*, 2003, **19**, 1357–1361.
26. S. S. Shankar, A. Ahmad, R. Pasricha and M. Sastry, *J. Mater. Chem.*, 2003, **13**, 1822.
27. S. S. Shankar, A. Ahmad and M. Sastry, *Biotechnol. Prog.*,**19**, 1627–31.
28. S. S. Shankar, A. Rai, A. Ahmad and M. Sastry, *J. Colloid Interface Sci.*, 2004, **275**, 496–502.
29. S. S. Shankar, A. Rai, B. Ankamwar, A. Singh, A. Ahmad and M. Sastry, *Nat. Mater.*, 2004, **3**, 482–8.
30. B. Ankamwar, C. Damle, A. Ahmad and M. Sastry, *J. Nanosci. Nanotechnol.*, 2005, **5**, 1665–1671.
31. B. Ankamwar, M. Chaudhary and M. Sastry, *Synth. React. Inorganic, Met. Nano-Metal Chem.*, 2005, 35, 19–26.
32. S. S. Shankar, A. Rai, A. Ahmad and M. Sastry, *Chem. Mater.*, 2005, **17**, 566–572.
33. A. Rai, A. Singh, A. Ahmad and M. Sastry, *Langmuir*, 2006, **22**, 736–41.
34. S. P. Chandran, M. Chaudhary, R. Pasricha, A. Ahmad and M. Sastry, *Biotechnol. Prog.*,**22**, 577–83.
35. J. Huang, Q. Li, D. Sun, Y. Lu, Y. Su, X. Yang, H. Wang, Y. Wang, W. Shao, N. He, J. Hong and C. Chen, *Nanotechnology*, 2007, **18**, 105104.
36. L. Rastogi and J.Arunachalam, *Adv. Mat. Lett., 4(7)*, 2013, 548–555.
37. N. Chanda, R. Shukla, A. Zambre, S. Mekapothula, R. R. Kulkarni, K. Katti, K. Bhattacharyya, G. M. Fent, S. W. Casteel, E. J. Boote, J. A. Viator, A. Upendran, R. Kannan and K. V Katti, *Pharm. Res.*, 2011, **28**, 279–91.
38. F. G. Bottone, S. J. Baek, J. B. Nixon and T. E. Eling, *J. Nutr.*, 2002, **132**, 773–8.
39. L. M. Knowles and J. A. Milner, *Carcinogenesis*, 2000, **21**, 1129–34.
40. E.-K. Park, K.-B. Kwon, K.-I. Park, B.-H. Park and E.-C. Jhee, *Exp. Mol. Med.*, 2002, **34**, 250–7.
41. K.-B. Kwon, S.-J. Yoo, D.-G. Ryu, J.-Y. Yang, H.-W. Rho, J.-S. Kim, J.-W. Park, H.-R. Kim and B.-H. Park, *Biochem. Pharmacol.*, 2002, **63**, 41–7.
42. P. Dasgupta and S. S. Bandyopadhyay, *Nutr. Cancer*, 2013, **65**, 611–22.
43. Coates John, *Encyclopedia of Analytical Chemistry: Interpretation of Infrared Spectra, A Practical Approach*, John Wiley & Sons Ltd, Chichester, 2000.
44. Hampton Carissa, Demoin Dustin and Glaser Rainer E., *Vibrational spectroscopy tutorial: Sulfur and Phosphorus*, Columbia, 2010.
45. G. P. Jose, S. Santra, S. K. Mandal and T. K. Sengupta, *J. Nanobiotechnology*, 2011, **9**, 9.
46. R. M. Zucker, E. J. Massaro, K. M. Sanders, L. L. Degn and W. K. Boyes, Cytometry. A, 2010, **77**, 677–85.

47. G. FRENS, *Nat. Phys. Sci.*, 1973, **241**, 20–22.
48. K. R. Brown, D. G. Walter and M. J. Natan, *Chem. Mater.*, 2000, **12**, 306–313.
49. X. Shi, D. Li, J. Xie, S. Wang, Z. Wu and H. Chen, *Chinese Sci. Bull.*, 2012, **57**, 1109–1115.
50. Z. Jiang, Z. Feng, T. Li, F. Li, F. Zhong, J. Xie and X. Yi, *Sci. China Ser. B Chem.*, 2001, **44**, 175–181.

Figure Captions

Fig. 1 Synthesis and UV- visible spectra of gold nanoparticles (a) GNP formed only by conventional method (citrate), D-GNP formed by different volumes of 50 mM DADS (I: with 2.5 µl, II: with 5.0 µl, III: with 10 µl, IV: with 15 µl). (b) UV-visible absorption spectra of D-GNPs (I, II, III and IV). Inset: Absorption spectra of GNP and D-GNP-IV showing their characteristic peaks at 529 nm and 554 nm respectively.

Fig. 2 Physical characterization of D-GNPs (a) Particle size distribution of gold nanoparticles prepared by 10 µl of 50 mM of DADS *i.e.,* D-GNP-III as measured by DLS. (b) Represents surface charge of D-GNP-III. (c) AFM images of gold nanoparticles prepared by D-GNP-III, showing (i) 2D and (ii) 3D views. (d) Represents TEM images of D-GNP-III.

Fig. 3 FTIR spectra of DADS and D-GNP FTIR spectra of DADS (black) and D-GNP-III (blue) scanned over a range of 450 cm^{-1} to 4000 cm^{-1} with a scanning resolution of 4 cm^{-1}.

Fig. 4 Stability of D-GNP in culture media (a) D-GNP-II and (b) D-GNP-III were incubated in RPMI medium 24 hours and then the particle size distribution was measured by DLS. (c) UV-visible spectra of gold nanoparticles after 24 hours where GNP shows absorption maxima at 532 nm and D-GNP-II and D-GNP-III show absorption maxima at 556 and 558 nm respectively.

Fig. 5 Biological activities of D-GNPs in human leukemic cell lines (a) cytotoxic effects of gold nanoparticles in U937 and K562 cells. U937 and K562 cells were treated with D-GNP-III for 24

hours. Cell viability was measured by Trypan blue dye exclusion assay where 50 μM and 100 μM of DADS, and maximum equivalent volume of GNP were also used. Viability for untreated cells was considered as 100% and data are presented as Mean ± SE. Internalization of D-GNPs in U937 cells were studied by confocal microscopic images of U937 cells (b) untreated control and (c) treated with 16.6 μM of D-GNP-III. The dark spots indicated by arrow are agglomerated D-GNPs 24h post-treatment. Apoptotic effect of D-GNPs in U937 cell-line as seen by fluorescence microscopic pictures of DAPI stained U937 cells (d) untreated, treated with (e) D-GNP-II and (f) D-GNP-III respectively whereas (g), (h) and (i) represent phase contrast microscopic pictures of untreated U937 cells, D-GNP-II and D-GNP-III treated U937 cells respectively. (j) Inter-nucleosomal DNA fragmentation of U937 cells (5×10^6) treated with GNP and different concentration of D-GNP-II and D-GNP-III for 24 hours was detected by ethidium bromide staining - in a 2% agarose TBE gel. Lane 1 represents DNA Ladder, lane 2: only cell, lane 3: HAuCl4, lane 4: GNP, lane 5: 15.16 μM of D-GNP-II, lane 6: 8.84 μMof D-GNP-II, lane 7: 28.6 μM D-GNP-III, lane 8: 16.6μM of D-GNP-III.

Fig. 6 Intrinsic fluorescence of D-GNP treated U937 cells. Confocal microscopic images of U937 cells treated D-GNPs. (a) and (c) represent the phase contrast pictures of untreated and 16.6 μM of D-GNP-III treated U937 cells respectively whereas, (b) and (d) show fluorescence images of untreated and 16.6 μM of D-GNP-III treated U937 cells respectively.(e-h) represent Z-scanning images of different section of U937 cells (mentioned in the figures) treated with 16.6 μM of D-GNP-III showing green fluorescence.

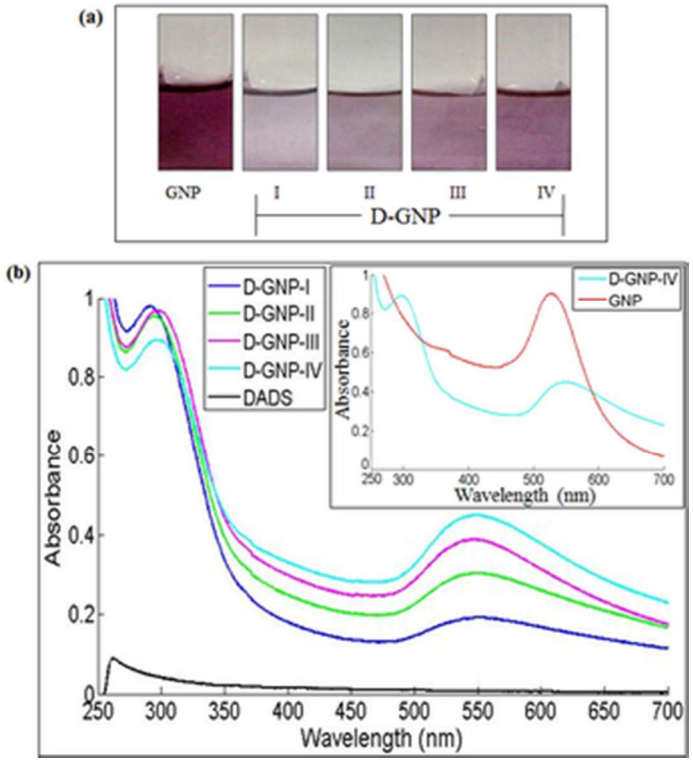

Figure 1
29x32mm (300 x 300 DPI)

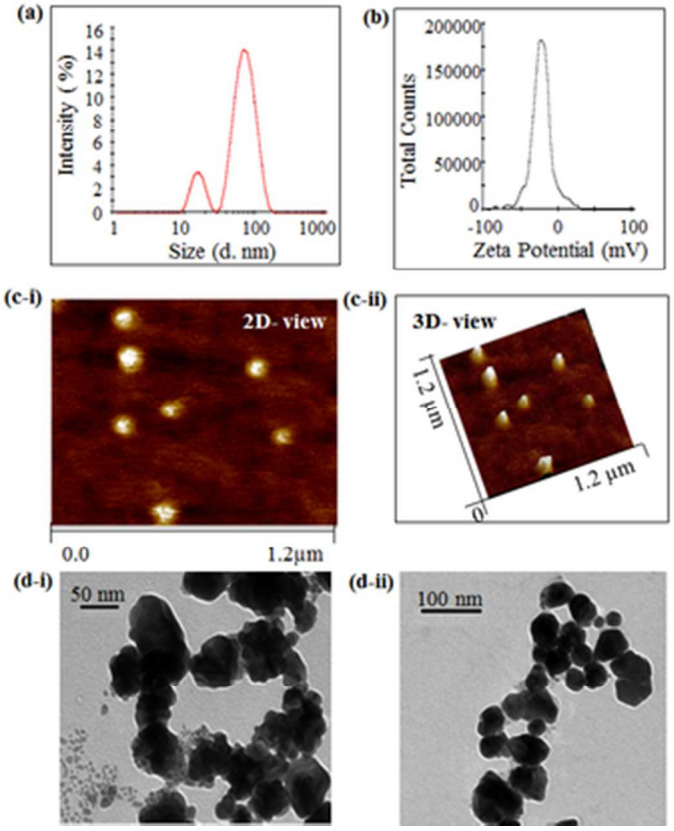

Figure 2
29x35mm (300 x 300 DPI)

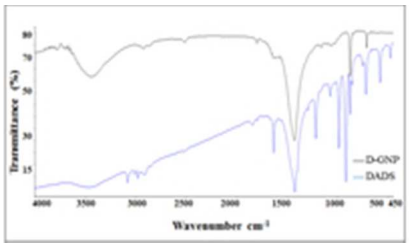

Figure 3
17x9mm (300 x 300 DPI)

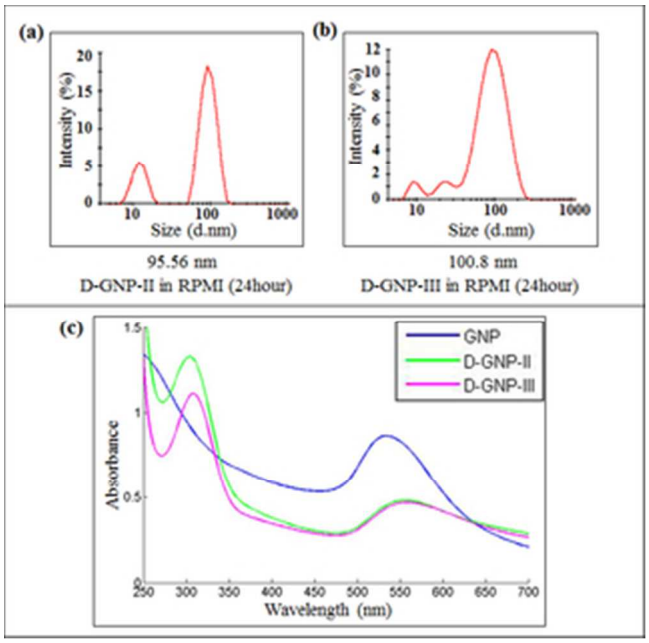

Figure 4
27x26mm (300 x 300 DPI)

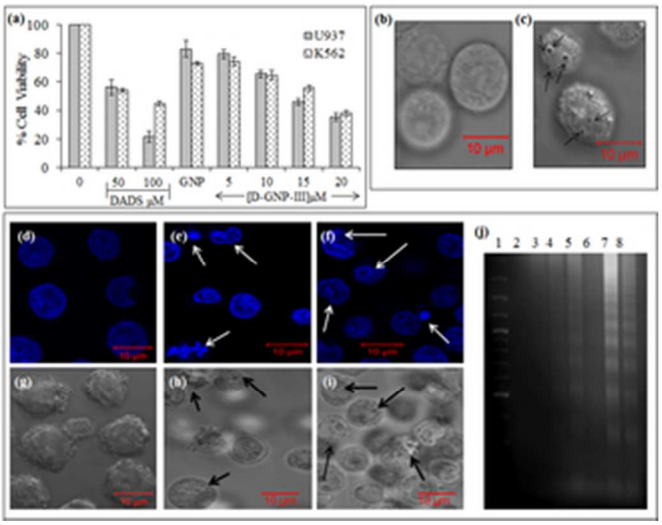

Figure 5
27x21mm (300 x 300 DPI)

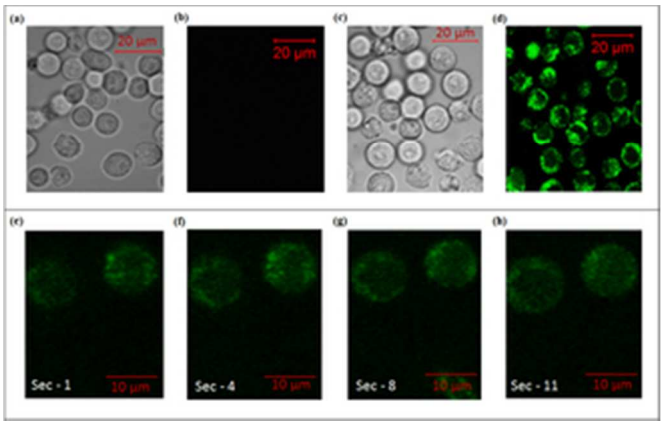

Figure 6
27x17mm (300 x 300 DPI)